

A tough nut to crack

J. S. JENNINGS, N. H. MACMILLAN

Materials Research Laboratory, The Pennsylvania State University, University Park, Pennsylvania 16802, USA

A study of the microstructure and mechanical properties of macadamia nutshells reveals these to behave like an "isotropic wood." Their dry density is $\sim 1.3 \times 10^3 \text{ kg m}^{-3}$, their Vickers hardness is $180 \pm 30 \text{ MPa}$, their fracture strength is 25 to 80 MPa and their fracture toughness is 1 to 2 $\text{MPa m}^{1/2}$. Their Young's modulus probably lies nearer the highest (6 GPa) than the lowest (2 GPa) of the present measurements and their work of fracture lies in the range 100 to 1000 J m^{-2} . None of the mechanical properties is obviously dependent on the water content of the shell. The results demonstrate quantitatively why these shells have a reputation for being difficult to crack.

1. Introduction

It is well known that the macadamia nut, which comes from an Australian evergreen tree (*Macadamia ternifolia*) of the protea family, is extremely difficult to extract from its shell. Perhaps less well known is that Patel [1] has obtained a patent for using a CO_2 laser to shell such nuts on a commercial scale. Curiosity about the mechanical properties of a material requiring such sophisticated technology to accomplish such a seemingly mundane task led the present authors to obtain several dozen freshly picked ("green") nuts and a similar quantity of dried ("dry-in-shell") nuts and to measure the Vickers hardness, Young's modulus, fracture strength, fracture toughness and work of fracture of their shells. This paper reports the results of the measurements, together with a variety of fractographic and microstructural observations.

2. Experimental materials and methods

2.1. Materials

Nuts were supplied by courtesy of Mauna Loa Macadamia Nut Corp. (Hilo, Hawaii 96720). They were approximately spherical, with an outer diameter of $\sim 2 \text{ cm}$ and a shell thickness of $\sim 2 \text{ mm}$. X-ray diffraction showed their shells to be completely amorphous. In the green condition the shells contained $\sim 22 \text{ wt } \%$ of water; and when dry-in-shell, i.e. after drying over a period of approximately three weeks at a temperature which was gradually raised from ambient to 333 K, their water content was 1.5 wt %. Pycnometry revealed their density to be $1.27 \times 10^3 \text{ kg m}^{-3}$ in this latter condition. In the green condition it approaches $1.5 \times 10^3 \text{ kg m}^{-3}$, which is the characteristic density of wood substance. To describe the orientation of a specimen, a simple geophysical analogy was adopted. The point of attachment of the nut to its parent tree was designated as the north pole and the suture was designated as the Greenwich meridian. According to this nomenclature the lining of the northern hemisphere is dark brown and that of the southern a pale yellow-white.

Figs. 1a and b are low magnification scanning elec-

tron micrographs of sections of dry shells which have been mounted in a low viscosity embedding medium (Spurr, Polysciences Inc., Warrington, Pennsylvania 18976) and wet-polished on 4000 grit SiC paper. Fig. 1a is a cross-section right through a shell in the plane of the equator and Fig. 1b is a similar cross-section from the equatorial region of the meridional surface exposed by bisecting a nut along a line of longitude. Cross-sections from the north and south polar regions of the same surface looked no different. Fig. 2a is a higher magnification micrograph of a portion of the microstructure shown in Fig. 1a, and Fig. 2b is a very high magnification micrograph from the north polar region of the section shown in Fig. 1b. Figs. 2c and d show corresponding sections through green shells at closely similar magnifications.

It is evident that the microstructure neither varies systematically with position within the shell nor exhibits any overall anisotropy. It consists of seemingly randomly oriented, irregularly shaped "bundles" of tens or hundreds of "rods" (cells). Within each bundle the rods are all more or less parallel and are packed together in an arrangement which approximates to close packing. The packing of the bundles fills space. A typical bundle is a few hundred micrometres in length and has an axial ratio ranging from one to five or larger. The individual rods consist of an inner core perhaps 5 to 25 μm in diameter surrounded by several concentric layers. Overall rod diameter is 15 to 40 μm . In both the green and the dry-in-shell conditions there is extensive microfracturing both between the component layers of individual rods and between adjacent rods. The opening displacement of these microfractures is somewhat greater in the dry-in-shell condition than in the green condition, but only rarely do they coalesce into larger intra-bundle or inter-bundle fractures in either condition.

2.2. Methods

2.2.1. Hardness

Measurements of the Vickers hardness H were made on the outsides of shells with a conventional Leitz

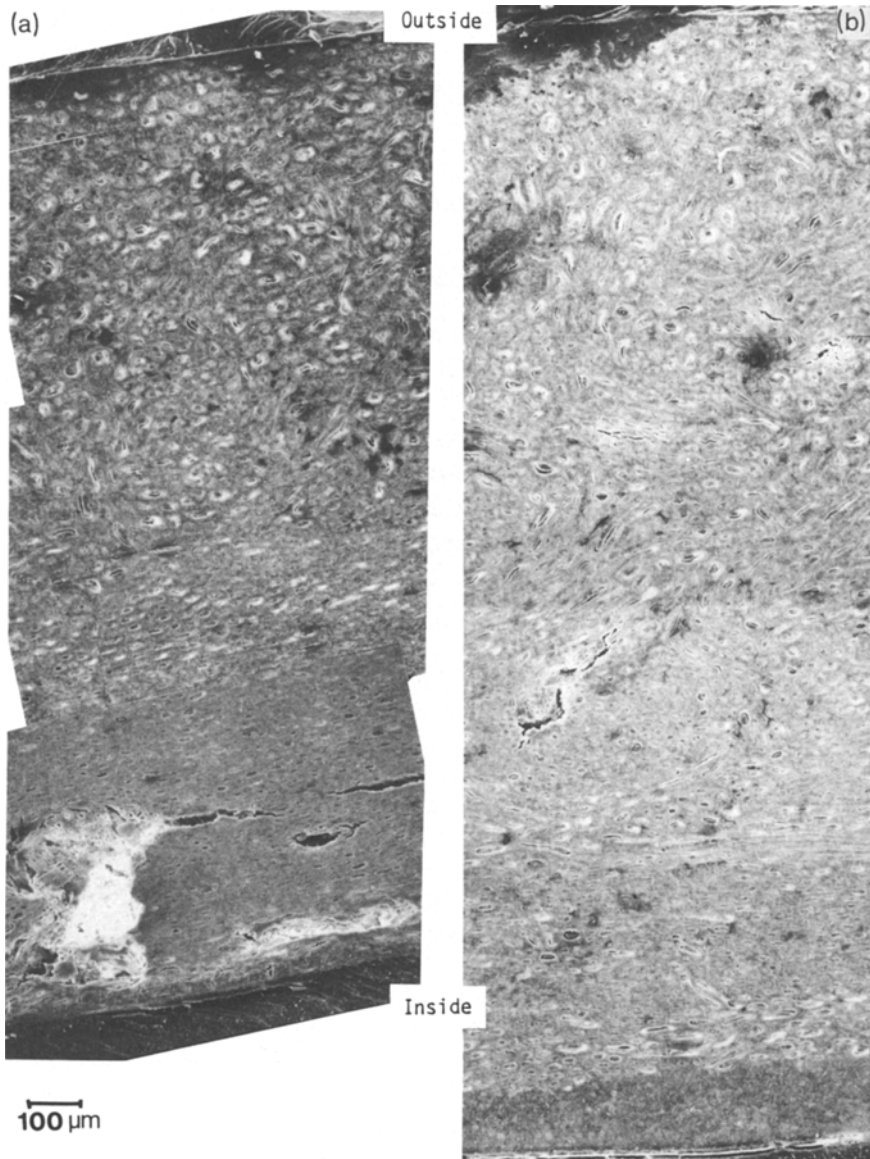


Figure 1 Polished cross-sections of dry shells (a) in the equatorial plane and (b) from the equatorial region of a meridional surface.

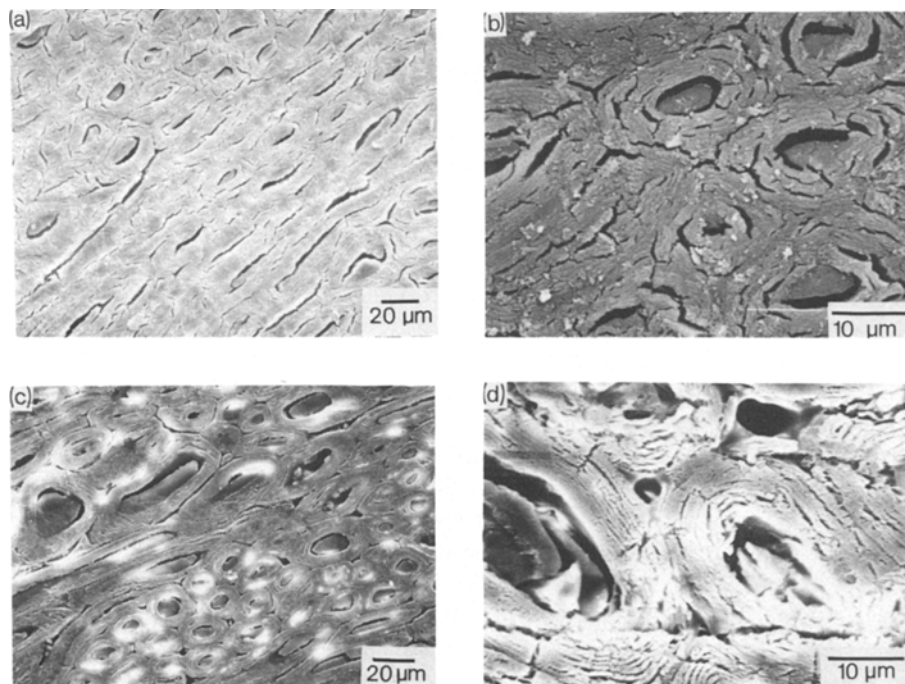


Figure 2 Polished cross-sections of shells from (a) an equatorial section of a dry shell at mid-thickness; (b) the north polar region of a meridional section of a dry shell at mid-thickness; (c) an equatorial section of a green shell at mid-thickness; and (d) the north polar region of a meridional section of a green shell at mid-thickness.

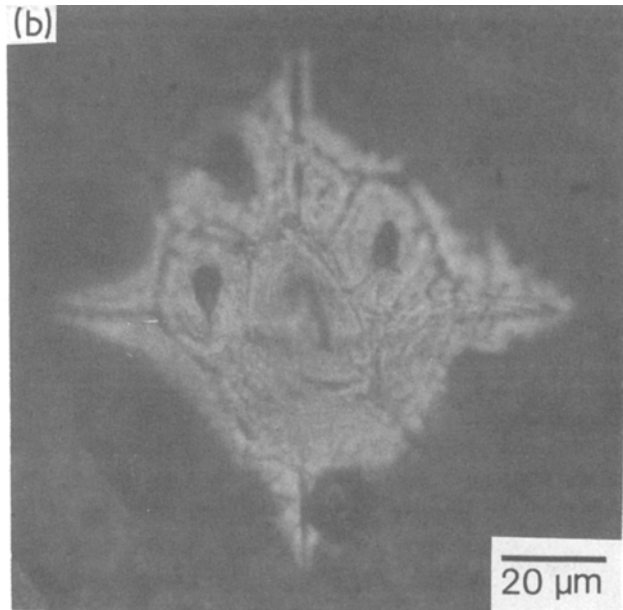
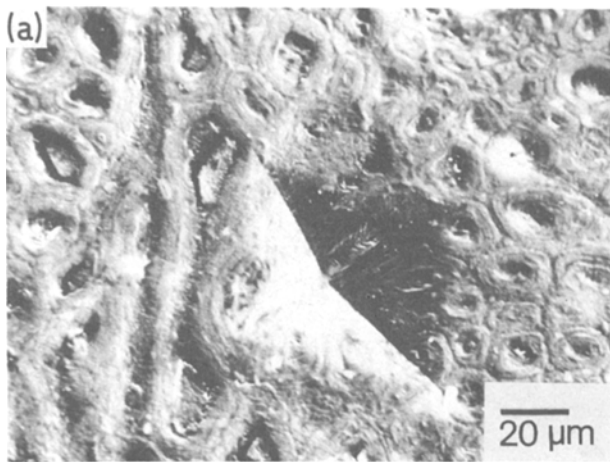


Figure 3 Vickers hardness impressions in the outer surfaces of (a) dry and (b) green shells. The effectiveness of the soot coating in enhancing the visibility of indentations is clearly apparent in the optical micrograph (b).

Miniload hardness tester, using a load of 100 g and a loading time of approximately 10 sec. The specimens were centimetre-dimension pieces of shell centred about five different locations – the north and south poles, latitudes 45° N and 45° S, and the equator. Each was prepared by: (i) mounting it with the area to be indented tangential to the top surface of a right cylinder of Koldmount resin (Vernon-Benshoff Co., Albany, New York 12201); (ii) lightly abrading it with 4000 grit SiC paper to create a millimetre-dimension flat “target” area; and (iii) passing it through the flame of a paraffin wax candle to coat it lightly with soot [2]. This procedure ensured that the load was applied radially to a flat surface held rigidly in the proper orientation and that the resultant indentations were clearly visible. The orientation of the indenter diagonals about the loading direction was varied at random relative to the lines of latitude and longitude passing through each indentation. Figs. 3a and b show, respectively, a scanning electron micrograph of an indentation in a dry piece of shell and an optical micrograph of one in a piece of green shell. Note that each indentation covers several rods.

2.2.2. Young's modulus and fracture strength

Young's modulus E and the fracture strength σ_f were determined from tensile and compressive C-ring tests [3] (Figs 4a and b) on specimens of two different orientations. Equatorial tensile specimens were prepared by removing an ~ 1 cm wide segment from a 5 to 7 mm wide, north–south geometrically symmetric annulus having the equator as its centre line; and the corresponding polar or meridional specimens were prepared by removing a similar segment from an east–west geometrically symmetric annulus of the same width which had as its centre line a line of longitude. The compression specimens were made by bisecting similar annuli. When necessary for accurate alignment with the loading system, small flats were ground on the outer surfaces of compression specimens where they came into contact with the loading platens. Similarly, it sometimes proved necessary to trim the inner edges of tension specimens to obtain proper alignment of the loading stirrups. All tests were performed on an Instron universal testing machine at a crosshead speed of 5×10^{-3} cm min $^{-1}$. The polar specimens were loaded along the polar diameter, and

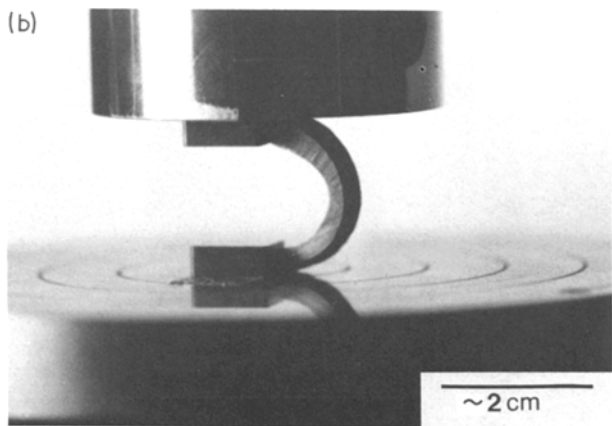
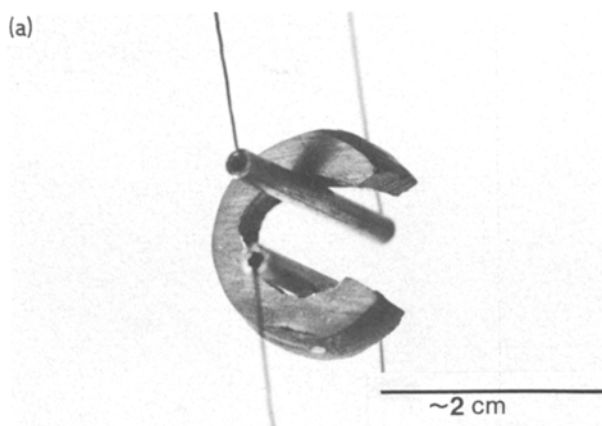


Figure 4 Experimental arrangements for performing C-ring tests (a) in tension and (b) in compression.

the equatorial specimens were loaded along an arbitrarily chosen equatorial diameter.

E and σ_f were calculated from linear isotropic elastic beam theory [3, 4]. If P is the applied load, x the displacement of the Instron crosshead, b the width of the annulus, and r_i and r_o the inner and outer radii of the shell,

$$E = \frac{3\pi(r_o + r_i)^3}{4b(r_o - r_i)^3} \frac{dP}{dx} \quad (1)$$

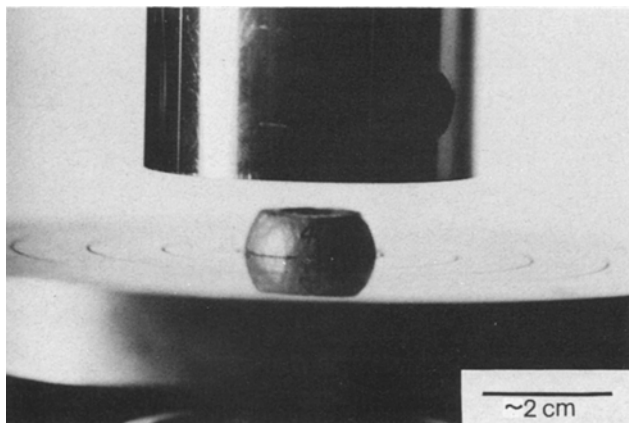
for a semi-circular beam-shaped specimen of rectangular cross-section when $(r_o + r_i) \geq 20(r_o - r_i)$. In the present work, $(r_o + r_i) \sim 10(r_o - r_i)$, but Equation 1 was nevertheless used to calculate E from the slopes dP/dx of the load–deflection curves in tension and compression because variation in specimen shape rendered more exact analysis inappropriate. In the same spirit, σ_f was also calculated as if the specimen was initially straight or only slightly curved, i.e. $(r_o + r_i) \geq 20(r_o - r_i)$. This allowed σ_f to be expressed to a sufficient approximation as the superposition of a uniform uniaxial tensile or compressive stress $P/b(r_o - r_i)$ produced by an axial load P and an inner or outer fibre tensile stress $3P(r_o + r_i)/b(r_o - r_i)^2$ produced by a bending moment $P(r_o + r_i)/2$, so that [3, 4]

$$\sigma_f = \frac{P}{b(r_o - r_i)} \left(\frac{3(r_o + r_i)}{r_o - r_i} + 1 \right) \quad \text{in tension} \quad (2a)$$

and

$$\sigma_f = \frac{P}{b(r_o - r_i)} \left(\frac{3(r_o + r_i)}{r_o - r_i} - 1 \right) \quad \text{in compression} \quad (2b)$$

A few measurements of fracture strength were also made by uniaxially compressing hemispheres from which a small cap had been removed (Fig. 5). The equatorially oriented specimens of this genre, which were compressed along the polar diameter, were bounded by the equator and either latitudes 45° to 60° N or 45° to 60° S; and those designated as polar (or meridionally) oriented, which were compressed along an equatorial diameter, were bounded by a great circle through the north and south poles (i.e. a line of longitude) and a 30° to 45° small circle centred at the pole of this great circle. If the specimen is treated as a thin



hemispherical shell truncated at a height h_o above its base diameter, this geometry generates [5] a tensile hoop stress σ_f parallel to the base and a compressive hoop stress σ' in the perpendicular direction. σ_f and $|\sigma'|$ increase with increase in height h above the base diameter according to

$$\sigma_f = \frac{P}{\pi(r_o^2 - r_i^2)[1 - 4h^2(r_o + r_i)^{-2}]} \quad (3a)$$

and

$$\sigma' = -\sigma_f \quad (3b)$$

The test is thus unsatisfactory in that the largest tensile stress occurs at the interface between the specimen and the upper loading platen, where $h = h_o$, leading to the possibility that the measured value of σ_f could depend upon the condition of the surface of this platen. Nevertheless, the simplicity of the test makes it a useful complement to the C-ring test.

To complete the fracture testing, a few complete shells were compressed uniaxially along either the polar or an equatorial diameter. It is difficult to obtain a meaningful fracture stress from the fracture load measured in such a test, because $\sigma_f \rightarrow \infty$ at the points of contact with the loading platens as $h_o \rightarrow r_o \simeq r_i$ in the approximation of Equation 3a. The result is nevertheless of interest because it defines the load which the consumer armed only with a conventional lever-action domestic nutcracker must apply to extract the nut from its shell.

2.2.3. Fracture toughness and work of fracture

Fracture toughness K_{Ic} was measured by means of notched C-ring tests which differed from the C-ring tests described in the previous subsection only in that each specimen was notched to a depth of a few tenths of a millimetre across its full width at its mid-length prior to testing. These notches were oriented perpendicular to the load axis and were placed in the inner surfaces of specimens tested in tension and the outer surfaces of specimens tested in compression. Some notches were “clean” cuts made with a sharp razor blade and others “ragged” cuts made with a fine saw-blade. The results obtained from specimens notched in these two different ways were not significantly different. K_{Ic} was calculated from the expression

$$K_{Ic} = 1.12\sigma_f(\pi c)^{1/2} \quad (4)$$

Figure 5 Experimental arrangement for testing truncated hemispheres.

TABLE I Vickers hardness of macadamia nutshells

Location	Hardness (MPa)	
	Green	Dry-in-shell
North pole	150 ± 20	200 ± 20
45° N	160 ± 20	180 ± 10
Equator	190 ± 10	210 ± 30
45° S	190 ± 10	190 ± 20
South pole	170 ± 20	180 ± 10

This is the condition derived from linear elastic fracture mechanics for propagation of a single-ended crack oriented perpendicular to the edge of a semi-infinite plate when the plate is loaded uniformly at infinity in uniaxial tension parallel to its edge. It is, however, an acceptable approximation for the fracture of an edge-cracked beam in bending when $(r_o + r_i) \gg (r_o - r_i)$ and the notch depth is much less than $(r_o - r_i)$ [6].

3. Results

All of the numerical data obtained are reported below as mean values plus or minus one standard deviation, as calculated from the results of six to twelve tests.

The results of the hardness tests are presented in Table I. They reveal that there is little variation in hardness with location over the shell and that there is no significant difference between the hardnesses in the green and dry-in-shell conditions. Nor did doubling or halving the load applied to the indenter affect the result obtained.

Table II shows that the uniaxial load required to crack a complete shell in diametral compression is indeed large enough to warrant the nut's reputation for being hard to crack. Even with the 3- or 4-to-1 mechanical advantage of the typical lever-action domestic nutcracker, it is difficult to generate manually the force required. Because of the sensitivity of this force to the precise shape of the shell at the point of loading, the fracture load data exhibit more scatter than the hardness data. Nevertheless, it appears that (like the hardness) this load depends neither on the orientation nor the water content of the shell. It is also worth noting that nuts compressed along the polar diameter exhibited no tendency to fail preferentially along the suture.

The values of Young's modulus, fracture strength, fracture toughness and work of fracture derived from the C-ring tests are presented in Table III; and Table IV presents the fracture strength data obtained by axially compressing truncated hemispheres.

Those C-rings tested in tension invariably fractured suddenly across the whole load-bearing cross-section at a clearly definable load, which thereupon fell to

zero; and some of those tested in compression behaved in the same way. For other compressed C-rings, however, the crack did not always propagate right through to the inner surface at the maximum load; and in these cases the load first dropped sharply to a small fraction of its maximum and then slowly fell to zero as the displacement increased. Regardless of these differences, σ_f was in all cases calculated from the maximum load.

In all sixteen conditions investigated (notched or un-notched, polar or equatorial orientation, green or dry-in-shell, tensile or compressive loading) the crack propagated more or less perpendicular to the load axis, and in all cases the fracture surfaces looked rather similar. Fig. 6 presents low magnification scanning electron micrographs of typical fracture surfaces produced under four different conditions: (a) notched, polar, dry-in-shell, compression; (b) un-notched, polar, dry-in-shell, tension; (c) un-notched, equatorial, dry-in-shell, compression; (d) un-notched, polar, green, compression. It appears that the fracture generally goes through rather than round the bundles of rods that make up the microstructure, and that the fracture surface is generally smoother at its inner and outer edges than near its centre, i.e. it is smoother in the regions of higher (tensile or compressive) stress far from the neutral axis. The higher magnification micrographs presented in Figs. 7a and b, which are blow-ups of the regions indicated in Figs. 6a and d, respectively, show further that the fracture path goes through the rods when these are more or less perpendicular to it, and between them when they lie more or less parallel to it. There is little evidence of "pull-out" of the cores of the rods. Fig. 7a also illustrates the dramatic difference in topography between a fracture surface and the surface of a sawn notch.

Interpretation of the compression tests performed on the truncated hemispheres was complicated by the fact that several fractures typically initiated at different points along the upper edge before any two developed sufficiently to permit a significant fraction of the specimen to spall away and terminate the test. The result was a "saw-tooth" load-displacement curve in which the tip of the first tooth did not necessarily represent the highest load supported by the specimen. Nevertheless, because of uncertainty about the stress distribution in the specimen after the formation of the first fracture, σ_f was in all cases calculated from the value of the load immediately before its first drop. In every case all fractures ran straight down the side of the specimen perpendicular to the tensile hoop stress; and in every case the crack passed through rods steeply inclined to its path and between rods lying more or less parallel to its path. Fig. 8 shows a portion of a fracture surface from a dry-in-shell equatorial specimen on which there is evidence of the occurrence of both processes.

When comparing the data summarized in Tables III and IV it is useful to keep in mind that equatorial C-rings and equatorial truncated hemispheres both fractured on meridional planes, that polar C-rings fractured in the plane of the equator, and that polar truncated hemispheres fractured on planes which

TABLE II Fracture loads for complete macadamia nutshells loaded uniaxially in diametral compression

Orientation of load	Fracture load (kN)	
	Green	Dry-in-shell
Equatorial	1.7 ± 0.5	2.4 ± 0.5
Polar (meridional)	1.7 ± 0.4	1.8 ± 0.2

TABLE III Young's modulus, fracture strength, fracture toughness and work of fracture of macadamia nutshells

Specimen orientation and mode of testing	Young's modulus (GPa)		Fracture strength (MPa)		Fracture toughness (MPa m ^{1/2})		Work of fracture (kJ m ⁻²)	
	Green	Dry-in-shell	Green	Dry-in-shell	Green	Dry-in-shell	Green	Dry-in-shell
Polar, tension	1.8 ± 0.8	3.7 ± 0.9	40 ± 6	65 ± 6	1.4 ± 0.4	1.8 ± 0.5	1.0 ± 0.5	0.8 ± 0.4
Polar, compression	5.2 ± 2.9	5.2 ± 4.2	51 ± 6	83 ± 15	0.8 ± 0.1	2.0 ± 0.9	0.12 ± 0.03	0.8 ± 0.7
Equatorial, tension	3.1 ± 2.8	4.9 ± 2.3	46 ± 11	46 ± 18	1.4 ± 0.5	1.4 ± 0.3	0.7 ± 0.5	0.4 ± 0.1
Equatorial, compression	6.0 ± 1.9	5.8 ± 1.9	56 ± 41	56 ± 17	0.9 ± 0.2	1.4 ± 0.2	0.13 ± 0.10	0.3 ± 0.1

could be inclined at any angle to the equatorial plane. Despite these differences, neither test yielded fracture strengths exhibiting any obvious and consistent anisotropy. Nor did either test provide any unequivocal indication that the fracture strength depends on moisture content. There is some indication from the C-ring tests that the polar-oriented dry-in-shell specimens were a little stronger and had a little higher fracture toughness, but this is not confirmed by the tests on the truncated hemispheres. What does seem clear is that the fracture strengths obtained by compressing truncated hemispheres are always a little lower than those obtained from C-ring tests, regardless of specimen orientation or moisture content. This difference may, however, be nothing more than a consequence of ignoring friction at the platen-specimen interfaces in the stress analysis leading to Equations 3a and b.

The data presented in Table III also suggest that Young's modulus is higher when the measurement is made in compression than when it is made in tension, particularly for the green specimens. Because these data were derived from the slopes of the load-displacement curves, the difference is doubtless due in part to the fact that the stirrups used to apply the tensile loads were more compliant than the anvils used to apply the compressive loads. This cannot be the whole story, however, for the same fixtures were used to test both the green and the dry-in-shell specimens, and the difference is much greater in the case of the former than of the latter. Nevertheless, it seems probable that the moduli measured in compression are more reliable than those measured in tension.

Since the work of fracture values G_{Ic} were calculated from the Young's modulus and the fracture toughness

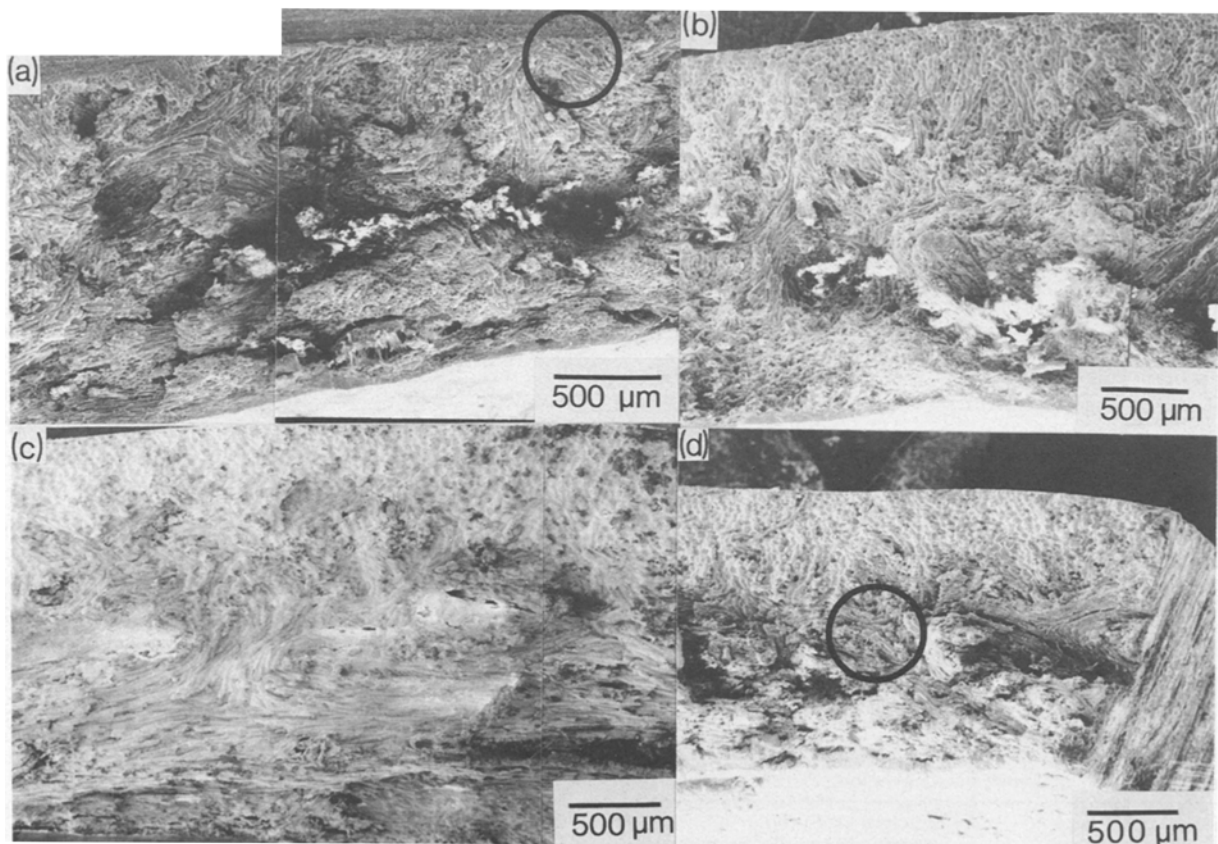


Figure 6 Fracture surfaces from C-ring tests in four different conditions: (a) notched, polar, dry-in-shell, compression; (b) un-notched, polar, dry-in-shell, tension; (c) un-notched, equatorial, dry-in-shell, compression; and (d) un-notched, polar, green, compression. Each figure is oriented with the outer surface of the shell at the top and the inner surface at the bottom. Rings indicate regions enlarged in Fig. 7.

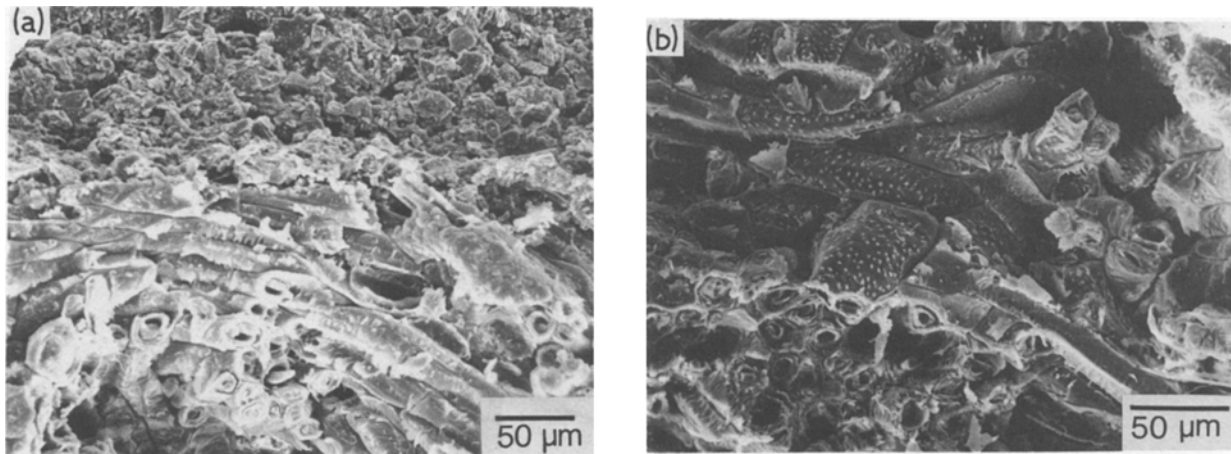


Figure 7 High magnification images (a) and (b) of the areas indicated in Figs. 6a and d, respectively. Note the difference between the sawn and fractured surface topographies at the top and bottom of (a).

data by means of the relationship [7]

$$G_{lc} = K_{lc}^2/E \quad (5)$$

they are subject to considerable uncertainty. In particular, the comparatively high values of G_{lc} quoted for green specimens tested in tension reflect the low values of Young's modulus obtained in the same condition. This suggests, albeit hardly conclusively, that macadamia nuts may exhibit a somewhat lower work of fracture in the green condition than when dry-in-shell, particularly when they are caused to fracture on the equatorial plane.

4. Conclusions

The mechanical properties of macadamia nuts are about what might be expected from their microstructure, i.e. the properties of an "isotropic wood." Spruce or fir or redwood, for example, has elastic moduli parallel and perpendicular to the grain of ~ 10 GPa [8, 9] and ~ 0.5 GPa [9], respectively. They also typically exhibit tensile strengths of ~ 100 MPa and ~ 5 MPa and compressive strengths of 30 to 50 MPa and 3 to 5 MPa in the same directions [8]. These values bracket the direction-independent moduli of 2 to 6 GPa and fracture strengths of 25 to 80 MPa measured in the present work. In similar fashion, the work of fracture measured in this work (0.1 to 1 kJ m^{-2}) lies between the values of ~ 0.1 and ~ 10 kJ m^{-2} typically measured for fracture along and across the grain of wood [10]. On the basis of specific strength or modulus (i.e. strength or modulus divided by density), however, the macadamia nutshell compares less favourably with such structural timbers because its density of $\sim 1.3 \times 10^3$ kg m^{-3} is 2.5 to 3 times that of spruce or fir or redwood (0.42 to 0.55×10^3 kg m^{-3} at 12 wt % moisture content [8]).

It is also interesting to compare the mechanical

properties of macadamia nutshells with those of common man-made materials. The results show these shells to have about the same Vickers hardness as annealed, commercial purity (1100-0) aluminium, which has almost exactly twice their density (2.7×10^3 kg m^{-3}); and they fracture at a stress that is about twice the yield strength and half the ultimate tensile strength of this metal. Though much softer than silicate glasses or any ceramic, they have about the same strength in tension as (say) soda-lime glass that has been handled without special precautions, and they are considerably stronger in tension than concrete or many coarse-grained, porous ceramics. Since the densities of silicate glasses range from 2.2 to 2.8×10^3 kg m^{-3} , and those of concrete, porcelain and domestic brick are $\sim 2.3 \times 10^3$, 2.3 to 2.5×10^3 and 1.4 to 2.2×10^3 kg m^{-3} , respectively, macadamia nutshells outperform all these materials on the basis of specific strength. Macadamia nutshells exhibit a fracture toughness (~ 1 $\text{MPa m}^{1/2}$) comparable with that of glass and many ceramics, but about an order of magnitude lower than that of a typical aluminium alloy; and their work of fracture (0.1 to 1 kJ m^{-2}) is about an order of magnitude higher than that of even a fully dense, high quality modern structural ceramic, although it is still two orders of magnitude below that of a typical

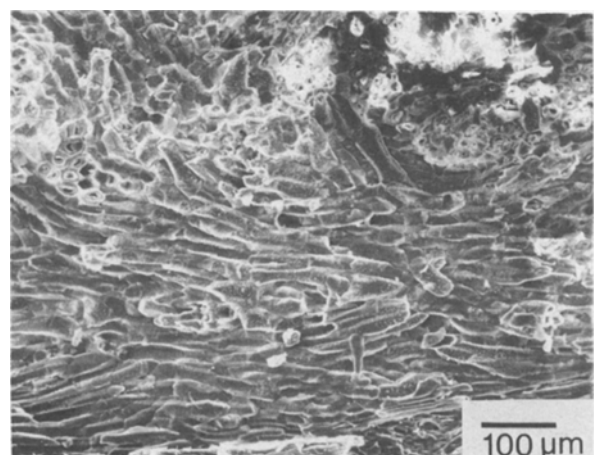


Figure 8 Fracture on a meridional plane produced by compressing an equatorially oriented truncated hemisphere cut from a dry shell.

TABLE IV Fracture strength of macadamia nutshells

Specimen orientation and condition	Fracture strength (MPa)
Polar, green	39 ± 19
Polar, dry-in-shell	25 ± 2
Equatorial, green	25 ± 6
Equatorial, dry-in-shell	24 ± 11

aluminium alloy. When its low elastic modulus (about one order of magnitude less than that of aluminium and nearly two orders of magnitude less than that of a modern structural ceramic) and even lower specific modulus are taken into account, the macadamia nutshell is seen to be a remarkably efficient and damage-tolerant structure. In the light of these data, it is no surprise that it is so difficult to crack open manually.

References

1. C. K. N. PATEL, US Patent 4358467 (1982).
2. N. H. MACMILLAN and D. G. RICKERBY, *J. Mater. Sci.* **14** 242 (1979).
3. J. R. G. EVANS and R. STEVENS, *Trans. J. Brit. Ceram. Soc.* **83** 14 (1984).
4. R. J. ROARK and W. C. YOUNG, in "Formulas for Stress and Strain", 5th Edn (McGraw-Hill, New York, 1975) pp. 89, 209.
5. S. TIMOSHENKO, in "Strength of Materials, Part II: Advanced Theory and Problems", 3rd Edn. (Van Nostrand, New York, 1956) p. 124.
6. B. R. LAWN and T. R. WILSHAW, in "Fracture of Brittle Solids" (Cambridge University Press, Cambridge, 1975) p. 58.
7. *Idem*, in "Fracture of Brittle Solids" (Cambridge University Press, Cambridge, 1975) p. 65.
8. "The Strength Properties of Timber", Forest Products Research Laboratory Bulletin No. 50, 2nd Edn. (HMSO, London, 1969) p. 14.
9. F. A. McCLINTOCK and A. S. ARGON, in "Mechanical Behavior of Materials" (Addison-Wesley, Reading, Massachusetts, 1966) p. 88.
10. G. JERONIMIDIS, in "The Mechanical Properties of Biological Materials", edited by J. F. V. Vincent and J. D. Currey (Cambridge University Press, Cambridge, 1980) p. 169.

*Received 26 February
and accepted 17 June 1985*